

Beyond Motion Imitation: Is Human Motion Data Alone Sufficient to Explain Gait Control and Biomechanics?

Xinyi Liu¹, Jangwhan Ahn¹, Edgar Lobato², Jennie Si³, He Huang¹

Abstract—With the growing interest in motion imitation learning (IL) for human biomechanics and wearable robotics, this study investigates how additional foot–ground interaction measures, used as reward terms, affect human gait kinematics and kinetics estimation within a reinforcement learning–based IL framework. Results indicate that accurate reproduction of forward kinematics alone does not ensure biomechanically plausible joint kinetics. Adding foot–ground contacts and contact forces to the IL reward terms enables the prediction of joint moments in forward walking simulation, which are significantly closer to those computed by inverse dynamics. This finding highlights a fundamental limitation of motion-only IL approaches, which may prioritize kinematics matching over physical consistency. Incorporating kinetic constraints, particularly ground reaction force and center of pressure information, significantly enhances the realism of internal and external kinetics. These findings suggest that, when imitation learning is applied to human-related research domains such as biomechanics and wearable robot co-design, kinetics-based reward shaping is necessary to achieve physically consistent gait representations.

Index Term— gait kinetics, reinforcement learning, imitation learning, biomechanics

I. INTRODUCTION

Imitation learning (IL), also known as learning from demonstrations, is a machine learning paradigm in which an agent learns a policy by observing demonstrations from an expert. The goal of IL is to reproduce a similar input–output behavior [1]. In the reinforcement learning (RL) formalism, RL-based IL typically seeks a policy that maximizes expected return under a reward function that explicitly encourages similarity to expert trajectories [2]. It offers a promising approach to capture the expert’s movement primitives and replicate demonstrated behaviors in forward dynamics simulations [3]. Recently, the rise of deep RL has enabled scalable policy representations that can mimic complex behaviors from raw sensory inputs, which has significantly advanced applications across various domains, including robotic manipulation [4, 5], physics-based animation [6, 7], autonomous driving [8, 9], humanoid control [10, 11], assistive systems [12, 13], etc.

¹ Joint Department of Biomedical Engineering, University of North Carolina - Chapel Hill, Chapel Hill, NC, USA Email: xinyili@ad.unc.edu, jahn26@ncsu.edu, hehuang@email.unc.edu

² Department of Electrical and Computer Engineering, North Carolina State University, Raleigh, NC, USA Email: ejlobato@ncsu.edu

³ School of Electrical, Computer and Energy Engineering, Arizona State University, Tempe, AZ, USA Email: si@asu.edu

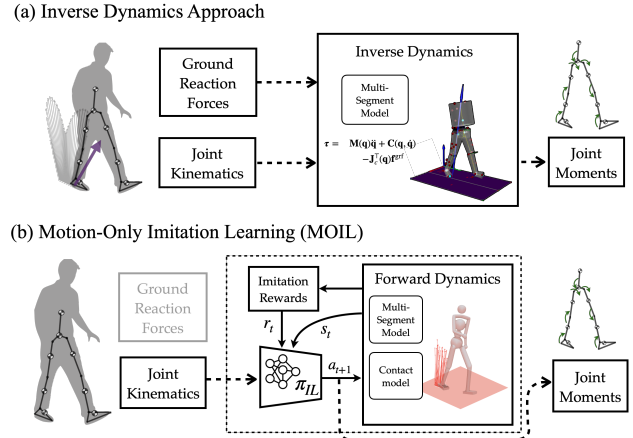


Fig. 1. Comparison of (a) a biomechanics inverse dynamics pipeline and (b) a motion-only imitation learning (IL) pipeline integrating a reinforcement learning agent with forward dynamics; ground reaction force measurements are omitted in MOIL approaches.

RL-based IL has recently attracted the attention of researchers in human biomechanics and wearable or rehabilitation robotics, since IL policies can reproduce expert demonstrated motions by generating the corresponding joint moments and even muscle activation patterns required for smooth, natural motion [6, 7]. In this study, we refer to these IL pipelines as the *motion-only IL* (MOIL). Retrospectively speaking, classic biomechanics analysis provides joint moment estimates from kinematics via inverse dynamics [14]. For locomotive tasks, given an approximate multi-segment dynamical model, joint kinematics from a motion capture system, and measured ground reaction forces (GRFs) from force plates or an instrumented treadmill, one can apply the Recursive Newton–Euler algorithm to compute biological joint moments, as shown in Fig. 1(a). Often, specialized instruments are required in the gait laboratory to collect these data for inverse dynamics calculation. In contrast, MOIL track joint kinematics or sparse task rewards without relying on external force measurements such as GRFs, as shown in Fig. 1(b). This approach is particularly appealing because measuring external forces is difficult in real-world and clinical settings, whereas human motion can now be measured ubiquitously, driven by rapid progress in wearable sensors and computer vision [15, 16]. MOIL may enable biomechanists, clinicians, and researchers to estimate joint kinetics and muscle activities without reliance on specialized force-sensing equipment, which is typically confined to gait laboratories [17]. This, in turn, could enable richer cause-

effect biomechanics analyses [18] and what-if analyses of responses to wearable robotic devices [19, 20], support clinically interpretable mobility assessments and diagnostic tools beyond the lab [21, 22], and facilitate co-design of shared-control wearable systems that generalize outside controlled clinical environments [23].

Focusing on walking, recent work has reported promising forward dynamics simulations of natural human gait using variants of MOIL [22, 24]. However, these studies rarely provide a systematic evaluation of the resulting GRFs and joint moments against experimental GRF measurements and inverse dynamics estimates. In cases where kinetics were reported [21, 25], the correspondence with inverse dynamics moment and force profiles is often incomplete or inconsistent across joints, tasks, or studies, making it difficult to conclude that the learned policies are *biomechanically plausible* in a robust and generalizable sense. A common observation from the forward dynamics simulation is the inaccurate magnitude and timing of foot-ground interaction forces and drift or bias in joint moments. Hence, questions remain regarding the usability and physiological validity of MOIL in biomechanics and human dynamic simulation.

Our central argument is that motion-only imitation learning alone may be insufficient to ensure the learning of policies that produce biomechanically plausible joint moments, even when the resulting forward dynamics simulations closely track the target kinematics within a small error margin. This is because RL can yield policies that produce targeted gait motion while relying on unrealistically altered foot-ground interaction, which would significantly deteriorate the joint kinetics estimates. We argue that additional expert knowledge of force-related measurements (e.g., GRFs and location of foot contacts) remains essential. To examine this hypothesis, we conducted an ablation study on an RL-based IL framework for normal walking. Specifically, we extended current MOIL [7] by introducing *kinetics-aware IL* (KAIL), which augments current motion imitation with additional rewards encouraging replication of external force measurements. By ablating the kinetics-related reward function that encourages imitation of either motion or foot contact measurements from a healthy person during walking, we trained policies to estimate joint kinetics and evaluated their biomechanical plausibility. Policy performance was assessed by comparing forward-simulated GRFs and joint moments against measured or inverse-dynamics-inferred values.

The outcome of this simulation study will inform researchers interested in using IL to build policies for estimating joint moments and muscle activations for biomechanical analysis, clinical diagnosis, and wearable robotics control design.

The remainder of this article is organized as follows. Section II introduces the biomechanical model, Section III formalizes the IL framework and reward design. Section IV details the experimental setup, data acquisition process, and the ablation scheme. Section V presents the learning performance and evaluation results. Section VI discusses the findings. Finally, Section VII concludes the study.

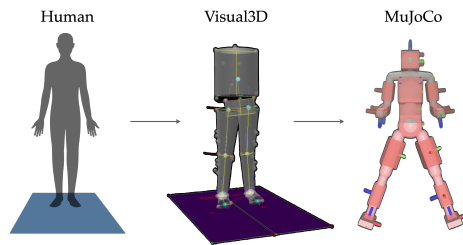


Fig. 2. Models used for the inverse dynamics and imitation learning. The Visual3D inverse dynamics model and the MuJoCo forward dynamics model shared identical anthropometric configurations (segment lengths, masses, and inertial properties) to ensure consistency.

II. HUMAN DYNAMICS MODELING

The human body is modeled as a floating-base, multi-segment system, as illustrated in Fig. 2. The system configuration is parameterized by the generalized coordinates $\mathbf{q} = [\mathbf{p}, q, \boldsymbol{\psi}]^T$, where $\mathbf{p} \in \mathbb{R}^3$ denotes the global root (pelvis) position, $q \in \mathbb{R}^4$ represents the root orientation quaternion and $\boldsymbol{\psi} \in \mathbb{R}^{17}$ defines the joint space coordinates. Specifically, the trunk is modeled as a single rigid segment connected to the root via a 3-DoF spherical joint, while each lower limb consists of a 3-DoF hip, a 1-DoF knee (flexion/extension), and a 3-DoF ankle joint. Forward dynamics simulations are implemented in MuJoCo [26], following the equations of motion for a constrained floating-base system.

$$\mathbf{M}(\mathbf{q}) \ddot{\mathbf{q}} + \mathbf{C}(\mathbf{q}, \dot{\mathbf{q}}) = \begin{bmatrix} \boldsymbol{\xi} \\ \boldsymbol{\tau} \end{bmatrix} + \mathbf{J}_c(\mathbf{q})^T \mathbf{f}^{\text{grf}}, \quad (1)$$

where $\dot{\mathbf{q}}$ and $\ddot{\mathbf{q}}$ are the generalized velocity and acceleration, $\mathbf{M}(\mathbf{q})$ is the generalized mass-inertia matrix, $\mathbf{C}(\mathbf{q}, \dot{\mathbf{q}})$ collects Coriolis, centrifugal, and gravitational terms, $\boldsymbol{\tau} \in \mathbb{R}^{17}$ denotes the actuated joint torques and $\boldsymbol{\xi} \in \mathbb{R}^6$ represent the corrective residual wrench applied to the floating base. Ground contact is represented through a set of holonomic constraints with Jacobian $\mathbf{J}_c(\mathbf{q})$, and \mathbf{f}^{grf} stacks the contact wrenches at the feet. Each foot is a box-shaped foot with four discrete contact points, and a contact layer is implemented via a contact margin $\epsilon = 0.05$ with contact time constant $\tau = 0.02$ and damping ratio $c = 1$, to obtain reasonably smooth foot-ground interactions.

III. LEARNING KINETICS

A. Problem Formulation

The IL problem is formulated as a finite-horizon Markov decision process (MDP) for a multi-segment dynamics model simulated in MuJoCo [26] and augmented with implicit residual forces following the RFC framework [7], as shown in Fig. 3.

1) *MDP Definition*: The RL environment defines an MDP $\mathcal{M} = (\mathcal{S}, \mathcal{A}, P, r, \gamma)$ with continuous state and action spaces. The policy operates on a state vector $\mathbf{s}_t = [\mathbf{q}_t^-, \dot{\mathbf{q}}_t^r, \phi_t]$ constructed from the simulated environment, consisting the generalized coordinates excluding the root global horizontal position $\mathbf{q}_t^- \in \mathbb{R}^{n_u+5}$, generalized velocities expressed in the root heading-aligned frame $\dot{\mathbf{q}}_t^r \in \mathbb{R}^{n_u+6}$, and the normalized

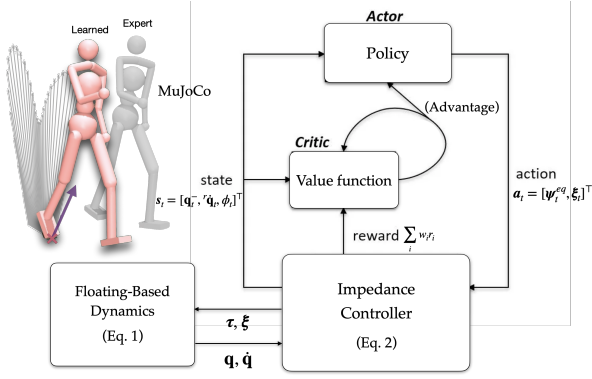


Fig. 3. Schematic of the actor-critic architecture for PPO-based residual-force control.

gait phase $\phi_t \in [0, 1]$. The action $\mathbf{a}_t = [\psi_t^{eq}, \xi_t]^\top \in \mathbb{R}^{n_u+6}$ concatenates equilibrium joint angle ψ_t^{eq} and residual wrench ξ_t . The transition to the next state \mathbf{s}_{t+1} is governed by the MuJoCo environment, simulating floating-based dynamics (Eq. 1) at 450 Hz over the policy's control interval $\Delta t = 1/30$ s, and the joint moments τ are generated by the impedance control law,

$$\tau = -\mathbf{K}_p(\psi - \psi^{eq}) - \mathbf{K}_d \dot{\psi}, \quad (2)$$

where \mathbf{K}_p and \mathbf{K}_d are the stiffness and damping coefficients as diagonal matrices. The equilibrium joint position ψ^{eq} is held constant throughout the control interval Δt ; likewise, the residual wrench ξ_t is held constant and applied to the root during the interval.

2) *Learning Objective*: Given an expert motion clip with generalized coordinate trajectory $\{\mathbf{q}_t^{\text{exp}}\}_{t=0}^T$, with corresponding GRFs $\{\mathbf{f}_t^{\text{grf-exp}}\}_{t=0}^T$ and center of pressure trajectory (CoP) $\{\mathbf{x}_t^{\text{cop-exp}}\}_{t=0}^T$, the goal is to learn a stochastic policy $\pi_\theta(\mathbf{a}_t | \mathbf{s}_t)$ that maximizes the expected cumulative reward

$$J(\theta) = \mathbb{E}_{\pi_\theta} \left[\sum_{t=0}^T \gamma^t r(\mathbf{s}_t, \mathbf{a}_t, \mathbf{q}_t^{\text{exp}}, \mathbf{f}_t^{\text{grf-exp}}, \mathbf{x}_t^{\text{cop-exp}}) \right],$$

where $\gamma \in (0, 1]$ is the discount factor, θ is the network variable, and the reward $r(\cdot)$ penalizes deviations between learned and expert kinematics, such as joint poses, end-effector positions, root motion, etc. On top of that, we also penalize deviations from the expert kinetic signals, as further explained in Section III-B.

B. Reward Design

The reward is decomposed into a kinematics-related term R^k and a kinetics-related term R^{dyn} , where

$$R^k = w^p R^p + w^{ee} R^{ee} + w^{\text{rp}} R^{\text{rp}} + w^{\text{rv}} R^{\text{rv}} + w^{\text{vf}} R^{\text{vf}}, \quad (3)$$

Here, R^k denotes the aggregated kinematic imitation objectives, following Yuan et al. [7]. The policy is encouraged to match the expert's joint kinematics (R^p), end-effector positions (R^{ee}), root orientation (R^{rp}), and root linear/angular velocities (R^{rv}). A residual-wrench regularization term (R^{vf}) penalizes excessive corrective wrench ξ_t , promoting dynamically feasible motion.

We further enforce *kinetics-aware* imitation by encouraging the match to the expert's GRF and CoP trajectories:

$$R^{\text{dyn}} = w^{\text{grf}} R^{\text{grf}} + w^{\text{cop}} R^{\text{cop}}, \quad (4)$$

where R^{grf} and R^{cop} are defined below.

- Ground reaction force (GRF) reward

$$R^{\text{grf}} = \exp\left(-k^{\text{grf}} \|\Delta \mathbf{f}^{\text{grf}}\|^2\right), \quad (5)$$

Here, $\Delta \mathbf{f}^{\text{grf}}$ stacks the difference of sagittal plane GRFs of learned interaction forces with the expert profiles from treadmill measurement,

$$\Delta \mathbf{f}^{\text{grf}} = [f_r^{\text{ap}} - f_r^{\text{ap-exp}}, f_l^{\text{ap}} - f_l^{\text{ap-exp}}, f_r^{\text{v}} - f_r^{\text{v-exp}}, f_l^{\text{v}} - f_l^{\text{v-exp}}]^\top,$$

where each term is the difference between learned and expert anterior–posterior (ap) or vertical (v) GRFs for the right (r) and left (l) feet at each time step.

- Center of Pressure (CoP) reward

$$R^{\text{cop}} = \exp\left(-k^{\text{cop}} \|\Delta \mathbf{x}^{\text{cop}}\|^2\right), \quad (6)$$

where similarly, $\Delta \mathbf{x}^{\text{cop}} = [x_r^{\text{ap}} - x_r^{\text{ap-exp}}, x_l^{\text{ap}} - x_l^{\text{ap-exp}}]^\top$ represents the difference between learned and expert anterior–posterior CoP position for the right and left feet. The CoP reward stabilizes contact dynamics by encouraging accurate distribution of pressure under each foot.

C. PPO Training Setup

The PPO controller was trained to imitate a motion-capture walking clip using a floating-based multi-segment whole-body dynamic model with a lumped upper body representation and an implicit RFC formulation [7] for dynamic compensation. The policy was modeled as a Gaussian stochastic actor with fixed action standard deviation $\exp(-2.3)$, implemented as a two-layer ReLU network with 512 and 256 hidden units. The value function used an identical architecture. Both networks were optimized using ADAM optimizer, with learning rates of 5×10^{-5} for the policy and 10^{-3} for the critic. Training employed Proximal Policy Optimization with clipping parameter $\epsilon_c = 0.2$ and generalized advantage estimation with discount factor $\gamma = 0.95$ and GAE mixing parameter $\tau = 0.95$. Each training iteration collected 50,000 environment steps, followed by 10 epochs of minibatch gradient updates with batch size 2048. Training ran for up to 900 iterations on an NVIDIA RTX A2000 GPU and an Intel i9-10900X CPU.

IV. EXPERIMENTS

A. Data Collection and Inverse Dynamics

We recruited one healthy young male (age: 29 years; height: 176 cm; mass: 70 kg) who had no history of musculoskeletal, orthopedic, or neurological diseases. The study protocol was reviewed and approved by the institutional review board (IRB No. 24671).

Forty-two reflective markers were placed on anatomical landmarks. Three-dimensional kinematic data were collected

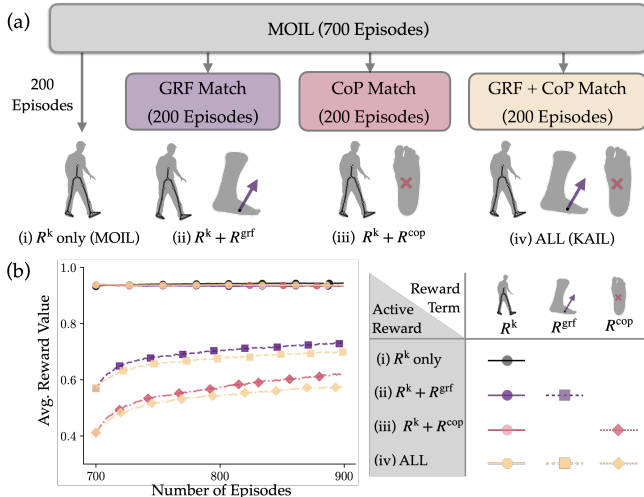


Fig. 4. Reward ablation scheme and corresponding reward curves. (a) Schematic of the training protocol, where agents are pre-trained with kinematic reward only (R^k) before entering a 200-episode fine-tuning phase under four conditions: (i) R^k only, (ii) R^k with GRF reward (R^{grf}), (iii) R^k with CoP reward (R^{cop}), and (iv) all terms combined. (b) Average reward values plotted individually for each reward component during the fine-tuning interval (700 to 900 episodes), corresponding to the active terms in each condition.

from the optical motion capture system (Vicon, Oxford, UK) at a sampling frequency of 120 Hz. GRFs were measured from the force-plate-embedded split-belt treadmill (Bertec, Columbus, OH, USA) at a sampling frequency of 1000 Hz. The participant completed a single 2-min trial of 1.2 m/s walking on a treadmill. We used the last 30 gait cycles for both the inverse dynamics and IL training.

Kinematics and GRFs data were filtered using a zero-lag fourth-order Butterworth filter with a cut-off frequency of 6 Hz and 10 Hz, respectively. Inverse kinematics and dynamics were performed in Visual3D biomechanical modeling software (HAS-Motion, Ontario, Canada). The gait cycle was defined from right heel strike to the subsequent ipsilateral heel strike using a 20 N vertical GRF threshold. Expert joint angles and GRFs were extracted from the last 30 gait cycles and time-normalized to 0–100% of the gait cycle.

B. Ablation Design

To evaluate the individual and combined contributions of the GRFs and CoPs reward terms to overall biomechanical plausibility, we conducted a systematic ablation study, as shown in Fig. 4(a). All models were initialized from the same pre-trained checkpoint (700 iterations), where MOIL successfully imitates expert’s walking motion (replicating the full trial without falls) to ensure a fair comparison, and were subsequently fine-tuned for an additional 200 iterations. The ablation systematically varied the kinetics-aware reward weights w^{grf} and w^{cop} during the last 200 iterations, while keeping all other hyperparameters fixed. Four training configurations were considered.

- 1) Baseline (R^k only), representing MOIL pipeline without any explicit kinetic supervision. The policy was

trained solely using the reward terms consistent with prior work in physics-based character animation and human motion imitation [7, 21].

- 2) GRF Matching ($R^k + R^{grf}$). To isolate the contribution of individual reward terms, explicit supervision was introduced on GRF tracking (Eq. 5). This condition examined whether aligning the foot–ground interaction forces is sufficient to recover physically plausible gait dynamics.
- 3) CoP Matching ($R^k + R^{cop}$). Similarly, supervision was applied individually to the CoP tracking reward (Eq. 6), isolating the effect of controlling the spatial location of ground contact forces.
- 4) Full pipeline (ALL), representing the full KAIL framework, including simultaneous supervision on both GRF and CoP signals.

V. RESULTS

A. Learning Performance

Fig. 4(b) shows the average reward for each reward term across the four conditions shown in Fig. 4(a) over episodes 700–900. In all four conditions, the policy completed the full walking trial without falls in forward dynamics simulations. The learning curve indicates that the kinematic reward component remains consistently within 0.93–0.95, with a maximum of 1 across all conditions, regardless of the addition of kinetics-aware rewards. The GRF reward increased from 0.55 to 0.71 in $R^k + R^{grf}$ condition. The CoP reward increased from 0.41 to 0.63, as shown in the left pane of Fig. 4(b). Finally, in ALL condition, the GRF reward and CoP rewards increased from 0.57 to 0.73 and from 0.41 to 0.59, respectively.

B. Kinematics Fidelity

Fig. 5(a) shows gait cycle normalized hip, knee and ankle joint angle profiles for the learned kinematics under the four conditions, along with experimental joint angle profiles. Fig. 5(b) presents the RMSE for each joint between each simulation learning condition and the averaged experimental profiles. The maximum RMSE was 6.56° in the knee joint for $R^k + R^{grf}$ condition.

C. External Kinetics Plausibility

We evaluated the alignment between simulated and measured GRF vectors in the sagittal plane during the stance phase. Fig. 6(a) shows GRF butterfly diagrams for the four learning conditions alongside the experimentally measured GRFs. Complex Pearson correlation coefficients (CPCC) were used to quantify the magnitude similarity between simulated and experimental GRF profiles. A paired t-test showed that correlations were significantly lower in the R^k only condition than in the conditions including kinetics-aware rewards (Fig. 6(b)) ($p < 0.001$). The statistical analysis also revealed that the R^k only condition exhibited significantly larger phase differences in GRF vectors compared with the other conditions ($p < 0.001$). Table I summarizes the CoP

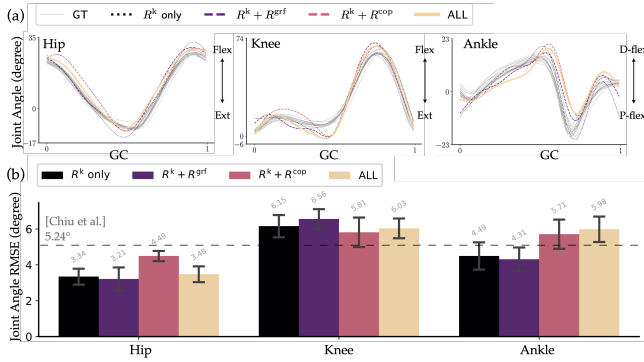


Fig. 5. Joint angle trajectories and tracking accuracy across ablation conditions. (a) Mean hip, knee, and ankle joint angles over the gait cycle (GC) for the forward-simulated kinematics generated from different ablation conditions. GT indicates ground truth kinematics trajectories. Flex and ext denote flexion and extension, respectively; D-flex and P-flex denote dorsiflexion and plantarflexion of the ankle joint, respectively. (b) The mean and standard deviation of joint angle RMSE for each joint and condition. A dashed horizontal line marks the reference error level reported by Chiu et al. [25]. Error bars denote standard deviations.

TABLE I. Statistical comparisons of anterior–posterior Center of Pressure (CoP) RMSE, normalized by foot length (FL), relative to the baseline condition (R^k only).

Condition	RMSE (% FL)	Reduction (%)	p -value
R^k only	38.3 ± 2.7	—	—
$R^k + R^{\text{grf}}$	32.8 ± 2.4	14.5	9.20×10^{-8}
$R^k + R^{\text{cop}}$	21.8 ± 2.4	43.2	2.75×10^{-12}
ALL	21.4 ± 2.3	44.3	4.78×10^{-12}

discrepancy in the anterior-posterior direction between the simulated and experimental CoP positions. The R^k only condition showed the highest RMSE. Adding the GRF reward reduced the error by 14.5% ($R^k + R^{\text{grf}}$) and CoP reward produced a 43.2% improvement ($R^k + R^{\text{cop}}$). The ALL condition yielded a 44.3% reduction. Paired t-tests revealed that in each case, including kinetics-aware rewards differed significantly from the R^k only condition ($p < 0.0001$).

D. Internal Kinetics Plausibility

Fig. 7 compares simulated joint moments with experimentally derived inverse dynamics reference moments. Simulated hip, knee, and ankle moment profiles are shown in Fig. 7(c). Pair-wise comparisons showed statistically significant reductions in RMSE for the hip, knee, and ankle moments when kinetic terms were included in the learning reward (Fig. 7(a)) ($p < 0.0001$). Pearson correlation coefficients further quantified waveform similarity (Fig. 7(b)), and paired t-tests indicated significantly stronger correlations at the hip for the $R^k + R^{\text{cop}}$ and ALL conditions than for the R^k only condition. For the knee and ankle, kinetics-aware conditions showed significantly higher correlations than the R^k only condition ($p < 0.0001$).

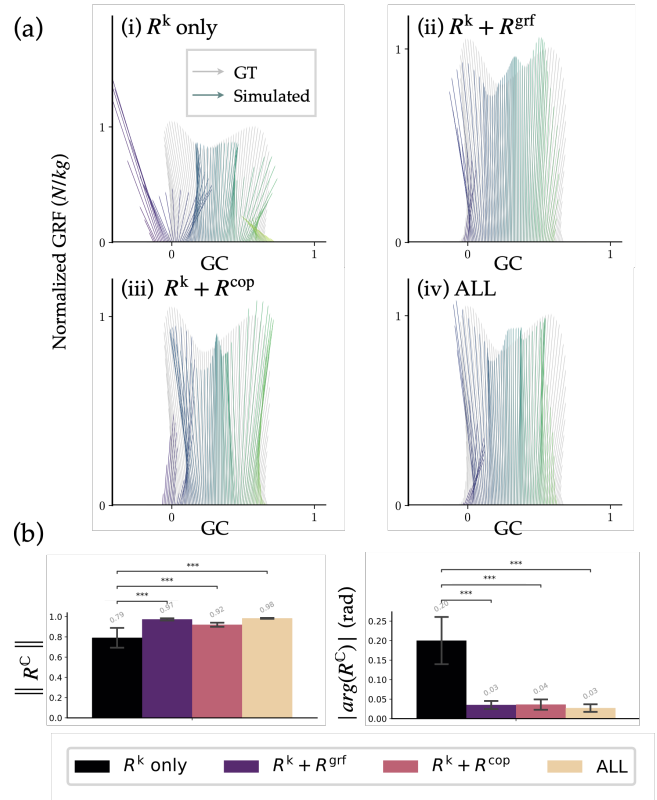


Fig. 6. Ground reaction force (GRF) vector trajectories and complex Pearson correlation coefficients (CPCC) analysis across reward function ablation conditions. (a) Sagittal plane GRF butterfly diagrams comparing forward-simulated GRFs with experimental GRFs (GT) across the ablation conditions; the color gradient and x-axis indicate normalized gait cycle (GC). (b) CPCC evaluation of GRF prediction accuracy: correlation magnitude ($\|R^C\|$) quantifies vector trajectory shape similarity, and absolute phase difference ($|\arg(R^C)|$) quantifies temporal misalignment. Error bars denote standard deviations, and asterisks indicate statistical significance ($*** p < 0.001$).

VI. DISCUSSION

In this study, we used IL to simulate normal human walking and conducted ablation studies on GRF/CoP reward terms' impact on gait kinematics and kinetics estimation. We found that both MOIL and KAIL agents could consistently produce desired gait kinematics across all reward formulations (Fig. 4(b)), with joint angle RMSE remaining within the acceptable error range for gait imitation reported by Chiu et al. [25] (Fig. 5).

However, MOIL rewards failed to ensure biomechanically plausible joint moments and GRFs. The learned gait exhibited impulsive heel strikes, inaccurate timing of contact events (Fig. 6), and large joint moment discrepancies (Fig. 7), consistent with previous studies [21, 25]. This failure can arise because MOIL may exploit the trade-off relationship between the stability and energy efficiency [27]. Specifically, MOIL can learn a simulation policy by allowing larger collision losses at heel strike to produce overly stable gait patterns, thereby prioritizing robustness over biological fidelity. However, this produces unphysiological GRFs which do not guarantee biomechanically plausible kinetics in human gait

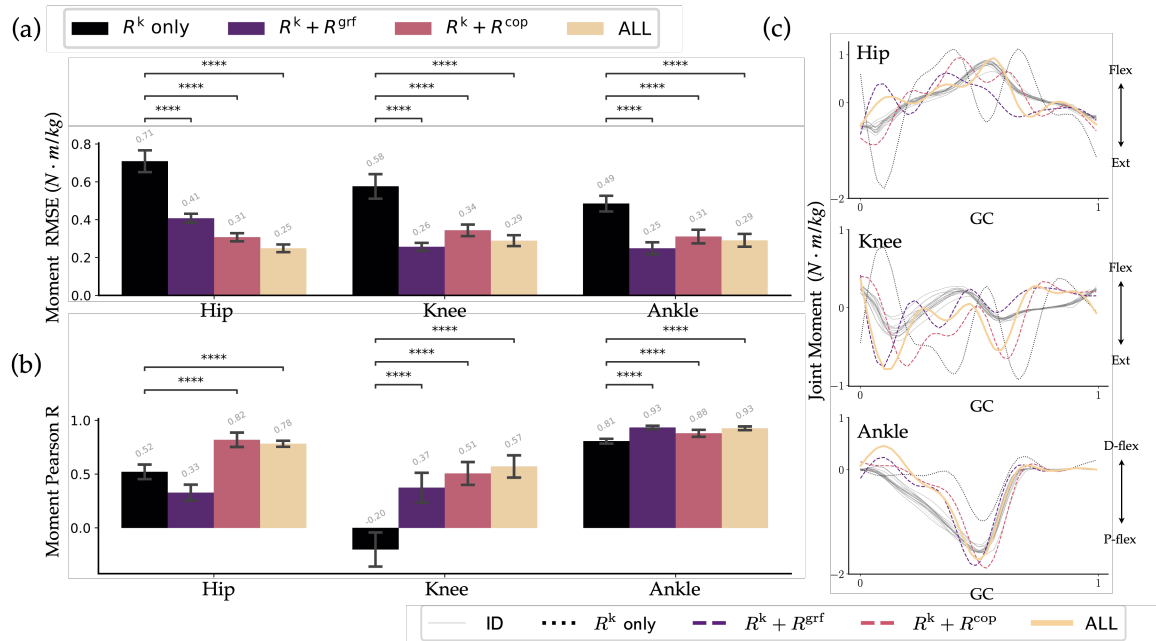


Fig. 7. Joint kinetics performance. (a) Joint moment estimation errors at the hip, knee, and ankle joints across ablation conditions. (b) Joint moment correlations with inverse dynamics joint moments at the hip, knee, and ankle joints across ablation conditions. (c) Joint moment trajectories comparing inverse-dynamics values (ID) over the gait cycle (GC) for each condition. Flex and ext denote flexion and extension, respectively; D-flex and P-flex denote dorsiflexion and plantarflexion of the ankle joint, respectively. Error bars denote standard deviations, and asterisks indicate statistical significance (**** $p < 0.0001$).

and can violate the dissipation range observed in human walking [28]. Meanwhile, KAIL produced more human-like kinetics by regularizing this tradeoff. Including foot-ground interaction measurements is necessary to estimate human-like joint moments in walking, as these constraints narrow the policy solution space to a physiologically realistic subset without compromising kinematic fidelity.

Foot-ground interactions play a critical role in human walking. Beyond the foot’s critical role as a sensory structure in gait [29], the foot-ground interface is mechanically indispensable in that the GRF’s magnitude, direction, and point of application at the foot fundamentally govern whole body walking dynamics [30]. Our results clearly demonstrate that better alignment of foot-ground interaction yields a better match to internal joint kinetics. Fig. 6 and Table I show that adding kinetics rewards produced GRFs that matched the measured GRFs significantly better in both magnitude and phase, and significantly reduced CoP location error relative to the R^k only condition. It has been shown that lower limb joint moment estimations from inverse dynamic analysis are sensitive to errors in the GRFs [31], and ~ 1 cm errors in anterior-posterior CoP location lead to $\sim 14\%$ errors in sagittal plane joint moment estimates [32]. Our joint moment estimates corroborate with these reports, as reduction of error in GRF and CoP through additional kinetics reward significantly reduced joint moment RMSE and increased correlation with the inverse dynamics biomechanics standards (Fig. 7).

It is noteworthy that by no means do we claim our KAIL pipeline fully reproduces human walking joint kinematics/kinetics. Even with GRF and CoP reward constraints,

KAIL-estimated moments still deviate from inverse dynamics analysis (Fig. 7). The IL-generated joint moments were jerkier than baseline kinetics, likely due to differences between model actuation dynamics and biological skeletal muscles. Human skeletal muscle behaves as a low-pass actuator [33], and standard musculoskeletal models adopt excitation-to-activation dynamics that suppress high-frequency force content [34]. In contrast, our model adopts an impedance controller with preset stiffness and damping coefficients following the previous open-source model [7], which yields joint moment profiles with a higher bandwidth and greater high-frequency content in the resulting joint moment. The error might also be derived from the inaccuracy in the foot-ground interaction model used in this study. For example, the noticeable errors in CoP trajectories can be observed. Among all the lower-limb joints, knee moments exhibited lower correlation than the other joints (Fig. 7(b)). Prior work indicates that knee moments are particularly sensitive to CoP location uncertainty [35]. Other modeling error sources, such as BSP matching errors, upper lumped body simplification, lack of neural control model, and soft tissue artifacts, may also contribute to the errors observed in kinetics estimation in this study. Nevertheless, it is important to note that the primary objective of this study is not to develop a fully biologically realistic walking model, but to assess whether motion imitation alone is sufficient for estimating gait kinetics in simulation. From this perspective, the presence of residual kinetic errors does not affect our central conclusion. The comparative results across reward formulations show that MOIL is fundamentally under-constrained for recovering biomechanically plausible

joint moments, whereas incorporating foot–ground interaction information systematically improves kinetic estimation.

Taken together, our findings call for a more cautious interpretation of recent enthusiasm surrounding MOIL for building “digital twin” models in human biomechanics or sim-to-real design of wearable robotics. Although MOIL has been successfully used in robotics and character animation for synthesizing control policies that reproduce desired human-like motions [6, 7, 36], these applications do not require production or interpretation of human-like joint moments. Nevertheless, when used for modeling humans or wearable robot design to reduce human muscle activity or energetic expenditures, the learned policy *must* mimic human musculoskeletal control for force production. This is because erroneous estimation of joint moments can lead to biased clinical diagnosis, rehabilitation strategies, or exoskeleton control policies. The inaccurate prediction of joint moments can further lead to incorrect estimates of muscle forces and activations during muscle force optimization. When the muscle activity is used to optimize wearable exoskeleton control, the biased estimation of muscle activation can be further coupled into wearable device control design, potentially degrading the intended rehabilitation assistance.

Hence, based on our research results, we advocated that rather than learning from motion only, accurate human dynamics modeling and kinetics inference would continue to require measurements of foot–ground interactions. Although inverse dynamics analysis estimates joint torques for a prescribed motion, IL-learned control policies remain invaluable for their ability to generate stable, coordinated, and continuous human movements in forward dynamics simulations. Through the stable walking simulation, one can (1) predict joint moments, loads, and muscle demands for clinical diagnosis purposes [21, 37]; (2) conduct cause-effect analysis and hypothesis testing [18, 38]; and (3) understand human–robot interaction and streamline the design of wearable robot control [20, 39, 25]. In this sense, IL should not be viewed just as a substitute for inverse dynamics analysis, but as a powerful simulation tool whose validity critically depends on how physical interaction constraints are incorporated.

Two primary limitations remain for this work that require future additional efforts. First, as discussed above, our simulation model still has errors. For instance, our foot–ground contact model remains an oversimplification, a known bottleneck in sim-to-real transfer [40]. Future work should investigate the joint optimization of the contact model and its parameters alongside policy learning to further reduce these kinetic discrepancies [41]. Second, this study evaluated only a single walking condition. Future work includes training policies across diverse terrains and walking speeds to ensure they can generalize and maintain balance under external perturbations. Addressing these modeling and generalization gaps will be essential for developing human models that are both stable and biomechanically accurate for biomechanics, rehabilitation devices, and clinical applications [19, 25, 39].

VII. CONCLUSION

This study aimed to evaluate how foot–ground interaction measures influence the gait kinematics and kinetics estimation through an RL-based IL framework. The primary finding was that accurate motion-only IL (MOIL) does not guarantee biomechanically plausible internal kinetics estimations. While the simulated motion matches observed gait patterns with or without kinetic reward constraints, the underlying joint moments may remain unrealistic without explicit kinetic regularization. Our results suggest that MOIL approaches are fundamentally limited to infer human-like joint dynamics, as they may prioritize kinematic trajectory matching over the physical consistency of force transmission. We argue that the biomechanically implausible joint moments represent a significant bottleneck for downstream applications of MOIL in biomechanics and lower-limb rehabilitation robotics. Our results demonstrate that incorporating kinetic constraints, specifically GRF and CoP location, in imitation learning (i.e., our KAIL framework) systematically improves the biomechanical plausibility of both external and internal kinetics. Future IL frameworks for human motion should integrate such measurements to ensure physical consistency and biomechanical plausibility.

REFERENCES

- [1] Brenna D Argall et al. “A survey of robot learning from demonstration”. In: *Robotics and autonomous systems* 57.5 (2009), pp. 469–483.
- [2] Tengpeng Zhang and Hongwei Mo. “Reinforcement learning for robot research: A comprehensive review and open issues”. EN. In: *International Journal of Advanced Robotic Systems* 18.3 (May 2021). Publisher: SAGE Publications, p. 17298814211007305. ISSN: 1729-8806. DOI: 10.1177/17298814211007305.
- [3] Maryam Zare et al. “A Survey of Imitation Learning: Algorithms, Recent Developments, and Challenges”. In: *IEEE Transactions on Cybernetics* 54.12 (2024), pp. 7173–7186. DOI: 10.1109/TCYB.2024.3395626.
- [4] Siheng Zhao et al. *ResMimic: From General Motion Tracking to Humanoid Whole-body Loco-Manipulation via Residual Learning*. 2025. arXiv: 2510.05070 [cs.RO].
- [5] Yuke Zhu et al. *Reinforcement and Imitation Learning for Diverse Visuomotor Skills*. 2018. arXiv: 1802.09564 [cs.RO].
- [6] Xue Bin Peng et al. “DeepMimic: Example-Guided Deep Reinforcement Learning of Physics-Based Character Skills”. In: *CoRR* abs/1804.02717 (2018). arXiv: 1804.02717.
- [7] Ye Yuan and Kris Kitani. “Residual force control for agile human behavior imitation and extended motion synthesis”. In: *Advances in Neural Information Processing Systems* 33 (2020), pp. 21763–21774.
- [8] Jianyu Chen, Bodi Yuan, and Masayoshi Tomizuka. “Deep Imitation Learning for Autonomous Driving in Generic Urban Scenarios with Enhanced Safety”. In: *2019 IEEE/RSJ International Conference on Intelligent Robots and Systems (IROS)*. Macau, China: IEEE Press, 2019, pp. 2884–2890. DOI: 10.1109/IROS40897.2019.8968225.
- [9] Jinning Li et al. “Guided Online Distillation: Promoting Safe Reinforcement Learning by Offline Demonstration”. In: *2024 IEEE International Conference on Robotics and Automation (ICRA)*. 2024, pp. 7447–7454. DOI: 10.1109/ICRA57147.2024.10611123.

- [10] Lujie Yang et al. *OmniRetarget: Interaction-Preserving Data Generation for Humanoid Whole-Body Loco-Manipulation and Scene Interaction*. arXiv:2509.26633 [cs]. Oct. 2025. DOI: 10.48550/arXiv.2509.26633.
- [11] Zhaoyuan Gu et al. “Humanoid locomotion and manipulation: Current progress and challenges in control, planning, and learning”. In: *arXiv preprint arXiv:2501.02116* (2025).
- [12] Hongjie Fang et al. *AirExo-2: Scaling up Generalizable Robotic Imitation Learning with Low-Cost Exoskeletons*. 2025. arXiv: 2503.03081 [cs.RO].
- [13] Liyiming Ke et al. “Grasping with Chopsticks: Combating Covariate Shift in Model-free Imitation Learning for Fine Manipulation”. In: *2021 IEEE International Conference on Robotics and Automation (ICRA)*. Xi’an, China: IEEE Press, 2021, pp. 6185–6191. DOI: 10.1109/ICRA48506.2021.9561662.
- [14] Kevin M Lynch and Frank C Park. *Modern robotics*. Cambridge University Press, 2017.
- [15] Kishor Das, Thiago de Paula Oliveira, and John Newell. “Comparison of markerless and marker-based motion capture systems using 95% functional limits of agreement in a linear mixed-effects modelling framework”. In: *Scientific Reports* 13.1 (2023), p. 22880.
- [16] Scott D Uhlich et al. “OpenCap: Human movement dynamics from smartphone videos”. In: *PLoS computational biology* 19.10 (2023), e1011462.
- [17] Abdul Aziz Hulleck et al. “Present and future of gait assessment in clinical practice: Towards the application of novel trends and technologies”. In: *Frontiers in medical technology* 4 (2022), p. 901331.
- [18] Seungmoon Song et al. “Deep reinforcement learning for modeling human locomotion control in neuromechanical simulation”. In: *Journal of NeuroEngineering and Rehabilitation* 18.1 (). Ed. by null. DOI: 10.1186/s12984-021-00919-y.
- [19] Nicholas A Bianco et al. “Simulating the effect of ankle plantarflexion and inversion-eversion exoskeleton torques on center of mass kinematics during walking”. In: *PLoS Computational Biology* 19.8 (2023), e1010712.
- [20] Yue Wen et al. “Automatically customizing a powered knee prosthesis with human in the loop using adaptive dynamic programming”. In: *2017 International Symposium on Wearable Robotics and Rehabilitation (WeRob)*. 2017, pp. 1–2. DOI: 10.1109/WEROB.2017.8383835.
- [21] R. James Cotton. *KinTwin: Imitation Learning with Torque and Muscle Driven Biomechanical Models Enables Precise Replication of Able-Bodied and Impaired Movement from Markerless Motion Capture*. en-US. arXiv:2505.13436 [cs]. May 2025. DOI: 10.48550/arXiv.2505.13436.
- [22] Pierre Schumacher et al. “DEP-RL: Embodied Exploration for Reinforcement Learning in Overactuated and Musculoskeletal Systems”. In: *The Eleventh International Conference on Learning Representations*. 2023.
- [23] Herman Van Der Kooij et al. “AI in therapeutic and assistive exoskeletons and exosuits: Influences on performance and autonomy”. en. In: *Science Robotics* 10.104 (July 2025), eadt7329. ISSN: 2470-9476. DOI: 10.1126/scirobotics.adt7329.
- [24] Firas Al-Hafez et al. *LocoMuJoCo: A Comprehensive Imitation Learning Benchmark for Locomotion*. arXiv:2311.02496 [cs]. Nov. 2023. DOI: 10.48550/arXiv.2311.02496.
- [25] Yi-Hung Chiu et al. “Learning Speed-Adaptive Walking Agent Using Imitation Learning with Physics-Informed Simulation”. In: *2025 International Conference On Rehabilitation Robotics (ICORR)*. 2025, pp. 835–841. DOI: 10.1109/ICORR66766.2025.11063216.
- [26] Emanuel Todorov, Tom Erez, and Yuval Tassa. “MuJoCo: A physics engine for model-based control”. In: *2012 IEEE/RSJ International Conference on Intelligent Robots and Systems*. 2012, pp. 5026–5033. DOI: 10.1109/IROS.2012.6386109.
- [27] Joeeun Ahn and Neville Hogan. “A simple state-determined model reproduces entrainment and phase-locking of human walking”. In: *PloS one* 7.11 (2012), e47963.
- [28] J.Maxwell Donelan, Rodger Kram, and Arthur D. Kuo. “Simultaneous positive and negative external mechanical work in human walking”. In: *Journal of Biomechanics* 35.1 (2002), pp. 117–124. ISSN: 0021-9290. DOI: [https://doi.org/10.1016/S0021-9290\(01\)00169-5](https://doi.org/10.1016/S0021-9290(01)00169-5).
- [29] Frederic JF Vieux. “The sensory role of the sole of the foot: Review and update on clinical perspectives”. In: *Neurophysiologie Clinique* 50.1 (2020), pp. 55–68.
- [30] Stephen J. Thomas, Joseph A. Zeni, and David A. Winter. *Winter’s biomechanics and motor control of human movement / Stephen J. Thomas, Joseph A. Zeni, David A. Winter (deceased)*. eng. Fifth edition. Hoboken, NJ: John Wiley & Sons, Inc., 2023 - 2023. ISBN: 9781119827023.
- [31] Rosa Pàmies-Vilà et al. “Analysis of different uncertainties in the inverse dynamic analysis of human gait”. In: *Mechanism and machine theory* 58 (2012), pp. 153–164.
- [32] Steven T McCaw and Paul DeVita. “Errors in alignment of center of pressure and foot coordinates affect predicted lower extremity torques”. In: *Journal of biomechanics* 28.8 (1995), pp. 985–988.
- [33] Skeletal Muscle In Vivo. “A Quantitative Evaluation of the Frequency”. In: *Journal of Biomechanical Engineering* 101 (1979), p. 28.
- [34] Jennifer L Hicks et al. “Is my model good enough? Best practices for verification and validation of musculoskeletal models and simulations of movement”. In: *Journal of biomechanical engineering* 137.2 (2015), p. 020905.
- [35] Franklin Camargo-Junior et al. “Influence of center of pressure estimation errors on 3D inverse dynamics solutions during gait at different velocities”. In: *Journal of applied biomechanics* 29.6 (2013), pp. 790–797.
- [36] Haotian Zhang et al. “Learning Physically Simulated Tennis Skills from Broadcast Videos”. In: *ACM Trans. Graph.* (). DOI: 10.1145/3592408.
- [37] Merkourios Simos, Alberto Silvio Chiappa, and Alexander Mathis. “Reinforcement learning-based motion imitation for physiologically plausible musculoskeletal motor control”. In: *arXiv* (2025). DOI: 10.48550/arXiv.2503.14637.
- [38] Seungmoon Song and Hartmut Geyer. “A neural circuitry that emphasizes spinal feedback generates diverse behaviours of human locomotion”. In: *The Journal of Physiology* 593.16 (2015), pp. 3493–3511. DOI: <https://doi.org/10.1113/JP270228>.
- [39] Visak C.V. Kumar et al. “Learning a Control Policy for Fall Prevention on an Assistive Walking Device”. en-US. In: *2020 IEEE International Conference on Robotics and Automation (ICRA)*. ISSN: 2577-087X. May 2020, pp. 4833–4840. DOI: 10.1109/ICRA40945.2020.9196798.
- [40] Leonor Saraiva et al. “A review on foot-ground contact modeling strategies for human motion analysis”. In: *Mechanism and Machine Theory* 177 (2022), p. 105046.
- [41] Claire V Hammond et al. “The Neuromusculoskeletal Modeling Pipeline: MATLAB-based model personalization and treatment optimization functionality for OpenSim”. In: *Journal of NeuroEngineering and Rehabilitation* 22.1 (2025), p. 112.